# Toroidally and Poloidally Localized ELMs

M. Hölzl[1], S. Günter[1], R.P. Wenninger[2], W.-C. Müller[1],
G.T.A. Huysmans[3], K. Lackner[1], I. Krebs[1], ASDEX Upgrade Team[1]

[1] *Max-Planck-Institut für Plasmaphysik, EURATOM Association, 85748 Garching, Germany*

[2] *Universitätssternwarte der Ludwig-Maximilians-Universität, 81679 München, Germany*

[3] *ITER Organisation, Route de Vinon sur Verdon, St-Paul-lez-Durance, France*

We use the non-linear MHD code JOREK to study ELMs in the geometry of ASDEX Upgrade. Toroidal mode numbers, poloidal filament sizes, and radial propagation speeds are in good agreement with experimental observations for type-I ELMs. The instabilities exhibit a localization compatible with "solitary magnetic perturbations" described in Reference [1]. Some of the results are presented in more detail in Reference [2].

## Simulations

Our simulations are carried out with the single-fluid reduced-MHD model of the JOREK code [3, 4]. Physical variables are poloidal flux $\Psi$, stream function $u$ (which also acts as electric potential), toroidal current density $j$, toroidal vorticity $\omega$, density $\rho$, temperature $T$, and velocity $v_{||}$ along field lines [5]. The poloidal plane is discretized by 2D Bezier elements [3], while a Fourier decomposition is applied toroidally. The temporal discretization is performed by a fully implicit second-order linearized Crank-Nicholson scheme [6]. The sparse system is solved by the GMRES-method with physics-based preconditioning.

The equilibrium of a typical ASDEX Upgrade H-mode discharge with type-I ELMs is used as starting condition (#23221@4.7s: $q_{95} = 4.7$, $P_{\text{heating}} = 9$ MW, $I_{\text{plasma}} = 1$ MA, $\beta_N = 1.6\%$) with plasma resistivities and viscosities increased versus the experimental values due to numerical limitations. Toroidal modes $n = 0 \ldots 16$ are resolved (periodicity 1). For comparison, cases with periodicities up to 8 (only $n = 0, 8, 16$) are also considered.

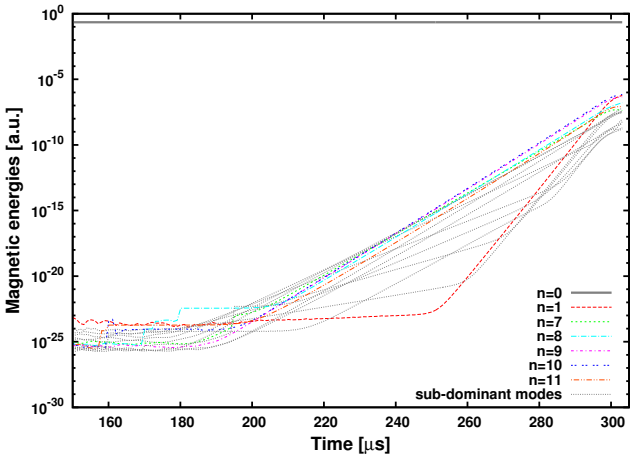


**Figure 1:** Magnetic energies are shown for the simulation with periodicity 1. The $n = 1$ mode non-linearly grows to a similar energy as the linearly most unstable $n = 10$ mode.

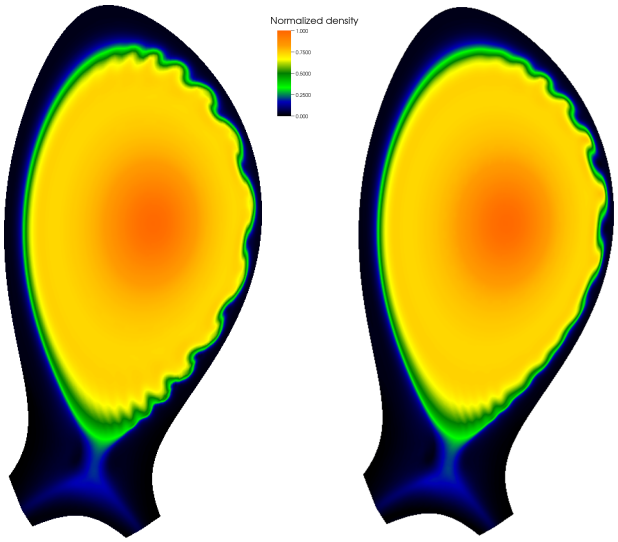


**Figure 2:** Density-perturbations are shown for periodicities 8 (left) and 1 at 294 µs. For periodicity 1, density-fingers are localized to the upper part of the outboard mid-plane at the poloidal plane shown.

## Results

The evolution of magnetic energies is shown in Figure 1. Linearly, the $n = 10$ mode has the largest growth rate $\gamma_{SI} \approx 2.0 \times 10^5$ s$^{-1}$. The initially very small growth rate of the $n = 1$ mode ($\gamma_{SI} \approx 2 \times 10^4$ s$^{-1}$) increases at $t = 150$ µs to $\gamma_{SI} \approx 4 \times 10^5$ s$^{-1}$ due to the interaction of $n_1 = 9$ and $n_2 = 10$ modes which may non-linearly drive $n_3 = \pm n_1 \pm n_2$ modes ($n_3 = 10 - 9 = 1$, in this case). In the non-linear phase of the instability, the $n = 1$ perturbation reaches a similar magnetic energy as the $n = 10$ perturbation which remains dominant also at the beginning of non-linear saturation ($t \approx 300$ µs). A first important effect that cannot be covered in simulations with high periodicity is the strong non-linear growth of low-$n$ modes. The growth rate of the dominant mode ($n = 10$ in our case) is not affected significantly by the toroidal mode-coupling. Also, the radial propagation velocity of the filaments into the vacuum region hardly changes compared to high-periodicity, the filaments accelerate up to a saturation level of about 3 km/s.

The density perturbation is shown in Figure 2. A ballooning-like structure is observed at the low-field side of the plasma. The poloidal size of ballooning-fingers is around $10 - 12$ cm at the mid-plane. Due to mode-coupling, not all fingers grow to the same amplitude at periodicity 1. A cluster of fingers can be seen that develops stronger than the rest of the ballooning-structures.

The localization becomes even more obvious when the magnetic footprint of the mode is considered. In Figure 3, the perturbation of $\Psi$ is plotted for different periodicities. Clearly, the localization of the mode can only be described correctly in simulations with periodicity 1.

Perturbations of all physical quantities are localized to a flux-tube like region close to the plasma edge which reaches from the vicinity of the lower (active) to the upper (inactive) X-point (Figure 3d). Strongest amplitudes are observed at the mid-plane, except for $v_{||}$ which is perturbed especially around the end-points of the flux-tube due to field-line stagnation. $\Psi$- and $j$-perturbations are located radially in the region of strong plasma current, while kinetic quantities are perturbed further outwards at the strongest pressure gradients.

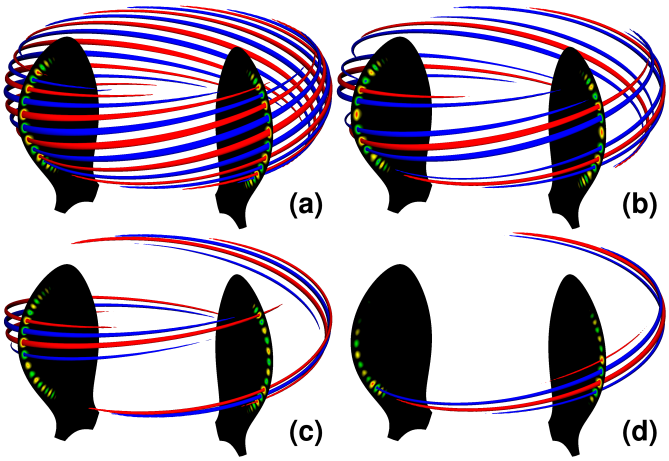


**Figure 3:** Poloidal flux perturbations are shown at periodicities **(a)** 8, **(b)** 4, **(c)** 2, and **(d)** 1. Red/blue contours are drawn at 70% min/max values. Strong localization is observed at small periodicities.

## Comparison to Experiments

Simulations with periodicity 1 exhibit a localization similar to solitary magnetic perturbations recently discovered in ASDEX Upgrade [1]. Toroidally asymmetric ELM-structures are also described in References [7–9]. Our instability does not show "explosive ballooning" shown found analytically in Reference [10].

Linearly, $n \approx 10-13$ dominates in our simulations, which is in reasonable agreement with experimental findings for type-I ELMs in ASDEX Upgrade and MAST, where $n = 8\ldots24$ was observed from energy deposition patterns [11], $n \approx 15$ using the mid-plane manipulator and visible-light imaging [12], and $n = 18 \pm 4$ was obtained from ECE-Imaging [13]. Uncertainties in our simulations come from limited resolution and neglect of diamagnetic stabilization (refer to Reference [2] for details).

Low-$n$ modes gain large amounts of energy non-linearly in our simulations. This should allow them to interact efficiently with core-MHD modes like tearing modes which typically also feature low toroidal mode numbers. There is experimental evidence from DIII-D that ELMs can be an important trigger for neoclassical tearing modes [14].

The poloidal filament-size at the midplane is around $10-12$ cm in our simulation. Sizes of $5-10$ cm are typically obtained for ASDEX Upgrade and MAST experimentally [12]. The deviation might result from simulated plasma resistivities and viscosities larger than in the experiment due to numerical limitations.

Radial propagation velocities increase and saturates at about 3 km/s in our simulations. In ASDEX Upgrade, a distribution around 1 km/s has been observed, where Filaments faster than 2 km/s occur in 20% of the cases and virtually no filaments faster than 3 km/s are observed [15, 16]. Hence, simulated and measured radial filament speeds agree reasonably well.

## Conclusions

Exponentially growing ballooning-like modes have been simulated with the reduced-MHD version of the non-linear MHD code JOREK in the geometry and using the profiles of a typical

ASDEX Upgrade H-mode discharge. Dominant toroidal mode numbers, poloidal filament sizes, and radial filament-propagation speeds are in good agreement with experimental observations for type-I ELMs in ASDEX Upgrade. At small periodicities, perturbations show a pronounced toroidal and poloidal localization compatible with solitary magnetic perturbations in ASDEX Upgrade. Low-$n$ modes are driven non-linearly in the simulations which might explain the interaction of ELMs with core-MHD modes reported in some experiments.

**Outlook**

In this article, we concentrate on the early ELM-phase. Further studies are planned to compare the simulation of a full ELM crash to experimental observations requiring a more sophisticated modelling of the scrape-off layer. Future numerical improvements and increased computational resources will be used to advance our investigations towards more realistic plasma parameters in simulations with periodicity 1.

**Acknowledgements**

Most simulations were performed on the HPC-FF cluster in Jülich, Germany. One of the authors (K.L.) would like to acknowledge support by the Austrian Science Fund (FWF) under grant No. P19901. Additionally, the authors would like to thank Erika Strumberger and Mike Dunne for help with equilibrium reconstruction and Klaus Reuter for help with visualizations.

**References**

[1] R. P. Wenninger, H. Zohm, et al. *Nuclear Fusion*. Accepted. URL http://arxiv.org/abs/1202.3603

[2] M. Hölzl, S. Günter, et al. *Phys. Plasmas*. Submitted. URL http://arxiv.org/abs/1201.5765

[3] O. Czarny and G. Huysmans. *Journal of Computational Physics*, **227** (2008), 7423 .

[4] G. Huysmans, S. Pamela, et al. In *Proceedings of th 23rd IAEA Fusion Energy Conference*. Daejon, South Korea (2010).

[5] H. R. Strauss. *Journal of Plasma Physics*, **57** (1997), 83.

[6] C. Hirsch. *Numerical Computation of Internal and External Flows, Volume 1, Fundamentals of Numerical Discretization*. Wiley (1989).

[7] H. Reimerdes, A. Pochelon, and W. Suttrop. *Nuclear Fusion*, **38** (1998), 319.

[8] M. Bécoulet, G. Huysmans, et al. *Plasma Physics and Controlled Fusion*, **45** (2003), A93.

[9] V. Bobkov, M. Becoulet, et al. In *Europhysics Conference Abstracts*, volume 28G (2004).

[10] H. R. Wilson and S. C. Cowley. *Phys. Rev. Lett.*, **92** (2004), 175006.

[11] T. Eich, A. Herrmann, and J. Neuhauser. *Phys. Rev. Lett.*, **91** (2003), 195003.

[12] A. Kirk, T. Eich, et al. *Plasma Physics and Controlled Fusion*, **47** (2005), 995.

[13] J. Boom, I. Classen, et al. *Nuclear Fusion*, **51** (2011), 103039.

[14] O. Sauter, R. J. L. Haye, et al. *Physics of Plasmas*, **4** (1997), 1654.

[15] A. Schmid, A. Herrmann, et al. *Plasma Physics and Controlled Fusion*, **50** (2008), 045007.

[16] A. Kirk, H. W. Muller, et al. *Plasma Physics and Controlled Fusion*, **53** (2011), 035003.